JTTEE5 21:255–262
DOI: 10.1007/s11666-011-9728-8
1059-9630/$19.00 © ASM International

Wettability of Atmospheric Plasma Sprayed Fe, Ni, Cr and Their Mixture Coatings

Zhengfeng Li, Yanjun Zheng, Jing Zhao, and Lishan Cui

(Submitted June 2, 2011; in revised form December 13, 2011)

Wetting behaviors of plasma sprayed Fe, Ni, Cr and their mixture coatings were investigated. The contact angle of water droplets on the surfaces increases with time when the surfaces are exposed to air, with the highest value greater than 150°. To the best of our knowledge, this is the first report that superhydrophobicity can be achieved by one step plasma spraying. It is found that the feedstock particle size distribution has a significant influence on the coating morphology. For the mixture coating, a micro/submicro dual scale roughness is obtained. The carbon content in the surface is found increasing with time. Results of X-ray diffraction, X-ray photoelectron spectroscope analysis and heat treatment in CO_2/Ar atmospheres suggest that the surface may contain some active ferrites which can decompose carbon dioxide into carbon. The origin of the superhydrophobicity is attributed to the accumulation of surface carbon materials and the dual scale roughness.

Keywords active ferrites, carbon material accumulation, dual scale structure, plasma spraying, superhydrophobicity

1. Introduction

As a fast and economical process for surface modification, atmospheric plasma spraying (APS) is often used to prepare various protective coatings for wear, erosion/corrosion and heat resistance (Ref 1–3). APS coatings are built up through successive deposition of the feedstock materials in a molten or semi-molten condition (Ref 1, 4). An ideal APS coating requires a dense, adherent and homogenous microstructure. However, depending on the nature of the coating process, many microdefects such as pores, microcracks and unmelted particles are often present in the coatings (Ref 5, 6). These microdefects can significantly affect the properties and performances of the coatings. During the past years, lots of works have been conducted on the microstructure and mechanical properties of APS coatings (Ref 1, 2, 6–11). However, as an important characteristic of solid surfaces, the wettability of APS coatings, especially APS metallic coatings, was rarely reported.

In industrial applications, APS coatings containing Fe, Ni and/or Cr have been extensively used. For example, stainless steel coatings (Ref 11) and Fe-based amorphous coatings (Ref 6) are often used in corrosive environments due to their excellent corrosion resistance and superior mechanical properties. Ni-based coatings have been widely used to protect steel structures such as turbine or boiler tube components from corrosion or high temperature oxidation (Ref 12). Recently, our group found that the wettability of a sprayed metallic Fe-Cr-Ni mixture coating can transform spontaneously from superhydrophilicity to superhydrophobicity. Moreover, this phenomenon was found having a good repeatability after plenty of repeated experiments. To the best of our knowledge, this is the first report of achieving superhydrophobicity on an APS metallic coating.

As we all know, the wettability of a surface is governed by the surface composition and surface morphology (microstructure). Superhydrophobicity needs a unique combination of these two factors (Ref 13, 14). In this paper, we attempt to explain the wettability change of the plasma sprayed metallic Fe-Cr-Ni mixture coating through investigating the composition and morphology of the surface. For comparison, the wettability change of pure metallic coatings prepared under the same conditions was also investigated. The results show that the superhydrophobicity of the Fe-Cr-Ni coating can be ascribed to its micro/submicro dual scale structure and high surface carbon content. Results of X-ray diffraction, X-ray photoelectron spectroscope analysis and heat treatment in CO_2/Ar atmospheres suggest that the iron particle after plasma spraying may form active ferrites, which can catalyze carbon dioxide into zero valence carbon.

2. Experimental

2.1 Materials and Spraying Process

All plasma spray powders were provided by Beijing General Research Institute of Mining & Metallurgy. The detailed information of each powder is listed in Table 1. A powder mixture with the ratio of Fe 40 wt.%, Ni 30 wt.% and Cr 30 wt.% were loaded in a stainless steel vial of

Zhengfeng Li, Yanjun Zheng, Jing Zhao, and **Lishan Cui**, Department of Materials Science and Engineering, China University of Petroleum, Beijing, China. Contact e-mail: zhengyj@cup.edu.cn.

300 mL in volume with hardened steel balls of 12 mm in diameter at a ball-to-powder weight ratio of 10:1, and then ball milled for 2 h at 600 rpm. All coatings were plasma sprayed onto copper plates with a dimension of $50 \times 50 \times 5$ mm^3 by using a DC plasma torch (APS-2000 K, China) with a nozzle diameter of 7.3 mm. Prior to spraying, the copper plates were thoroughly ultrasonically cleaned with acetone and distilled water, dried by compressed nitrogen gas, and then sand blasted. The plasma spray conditions are shown in Table 2.

2.2 Characterization of Coatings

The microstructure and elemental distribution of coatings were observed by using a FEI Quanta 200 scanning electron microscope (SEM) equipped with an energy dispersive X-ray spectrometer (EDX). The elemental and chemical compositions of the coatings were analyzed by X-ray photoelectron spectroscope (XPS, PHI Quantera SXM). The oxidation products were analysed using a D/max-2500 V X-ray diffractometer (XRD) with Cu-Ka radiation generated at 40 kV and 200 mA. The Contact angles (CA) and the sliding angles (SA) were measured by the sessile-drop method with distilled water (5 μL) on a DataPhysics OCA20 CA system at room temperature. A CA value was obtained by the average of at least five values at different positions of the same sample.

3. Results and Discussion

3.1 Wettability Change of APS Metallic Coatings with Time

Immediately after plasma spraying, water droplets are found to wet all the metallic coatings completely. The CA value, however, increases with exposure time to air, as shown in Fig. 1(a). The CA change rates and peak values are different for different coatings, wherein the mixture coating has the highest change rate and peak CA value. These results were found to have a good repeatability. It is worth noting that the contact angle and the sliding angle of the mixture coating have reached greater than 150° and lower than 5°, respectively, after exposed to air for 35 days, as shown in Fig. 2(a). The water droplets on such a surface have nearly spherical shapes (Fig. 2b), which can drip off rapidly when the surface is slightly inclined. These results indicate that the surface of the sprayed metallic Fe-Ni-Cr coating is superhydrophobic, which has a wide range of applications in many fields (Ref 13–15).

Generally, thermal spray coatings are used after polishing its surface. For comparison, we also investigated the wettability of the polished surfaces. The surfaces were prepared using wet grinding until 1200 grit SiC paper, and then ultrasonically cleaned in acetone, washed in distilled water and dried in air. The results are shown in Fig. 1(b). It can be seen that the contact angle of all coatings increases rapidly in the initial 12 days, and then the value stays almost constant for the following days. These results are similar to some previous reports (Ref 16, 17), where they attributed this phenomenon to the adsorption of organic substances from the atmosphere. The CA change rates and peak values of the rough surfaces and the

Table 1 Parameters of the spayed powders

Powder	Size, μm	Purity, %
Fe	≤40	>98.5
Cr	≤40	>99
Ni	≤75	>99

Table 2 Spray parameters

Classification	Condition
Plasma current	440 A
Plasma voltage	44 V
Primary gas flow rate	Ar: 40 L/min
Secondary gas flow rate	H_2: 10 L/min
Carrier gas flow rate	6 L/min
Powder feeding rate	20 g/min
Spray distance	100-120 mm

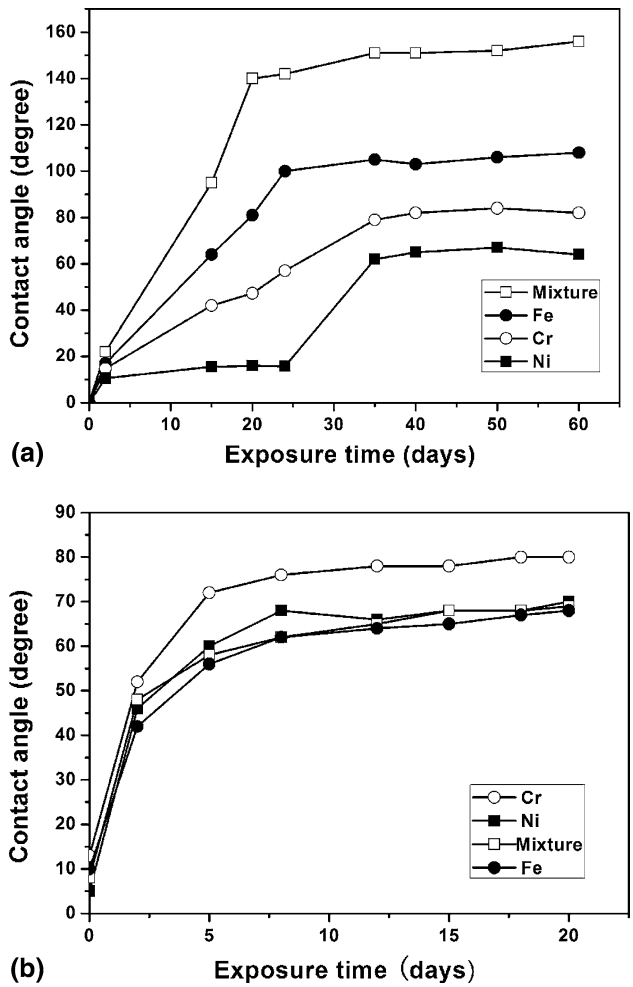

Fig. 1 The evolution of contact angle of water droplets over time on the prepared coatings with a rough surface (a) and a polished one (b)

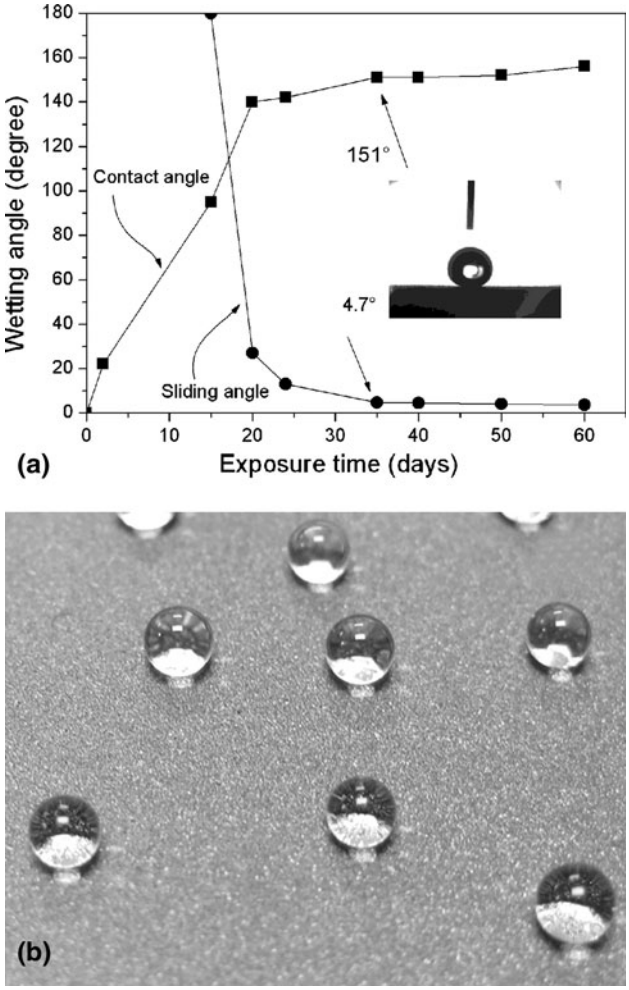

Fig. 2 (a) The evolution of contact angle and sliding angle over time on the sprayed mixture coating (the sliding angle 180° means that a water droplet can not roll off even when the surface is upturned). The inserted picture is a typical example of a droplet with a volume of 5 μL on the coating surface which has been exposed in air for 35 days. (b) A camera picture of water droplets sitting on the superhydrophobic surface

polished surfaces are different, which may be correlated to their surface composition and roughness, as we will discuss later.

3.2 Surface Characterization Shortly After Spraying

Figure 3 shows the surface composition of the prepared mixture coating shortly after spraying (no more than 5 h). From the EDX and XPS results we can see that the prepared coating surface contains a large number of oxides, which indicates that the metal powders have suffered severe oxidation during air plasma spraying. In addition, a small amount of carbon element (~16.8 at.%) was detected in the surface. The carbon may come from the organic substances adsorbed from the air (Ref 16, 17), because the sample was exposed to air for some short time period (no more than 5 h) between the plasma spraying and XPS analysis.

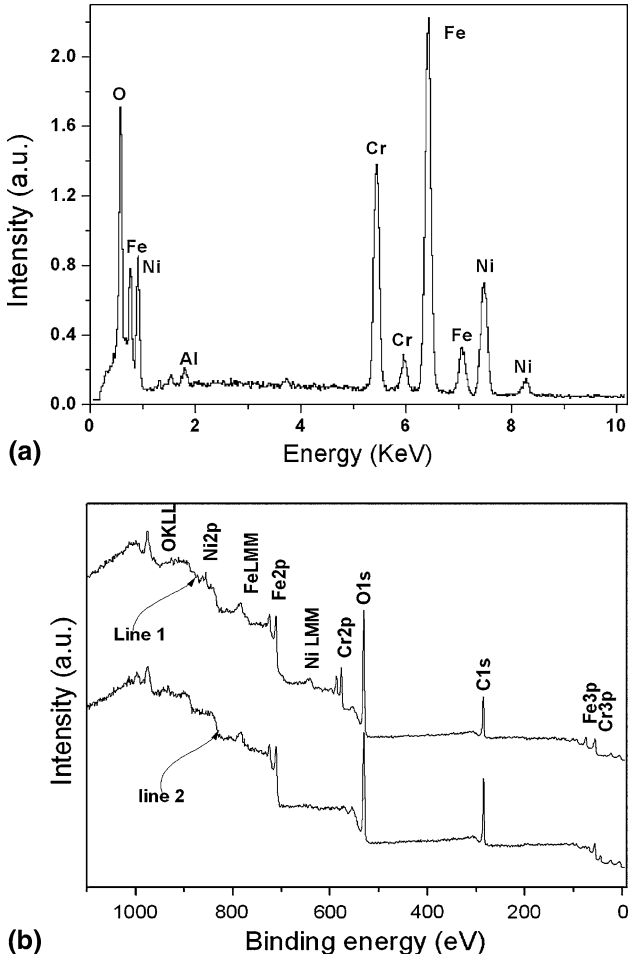

Fig. 3 (a) The EDX spectrum of the sprayed mixture coating. (b) XPS spectra of the coating. Line 1 is obtained 5 h after the spraying process, and line 2 is obtained 35 days after the spraying process

The morphology (microstructure) of the mixture coating is shown in Fig. 4. As can be seen in Fig. 4(a), islands of 20-40 μm in diameter with an average distance of about 20-50 μm are distributed across the surface. Figure 4(b) is the magnification of a local area in Fig. 4(a), showing numerous smaller particles spread over the large islands. This dual scale structure is very similar to the morphology of lotus leaf which has a micro/nano binary structure (Ref 14). Moreover, from the cross-section morphology shown in Fig. 4(c), we can see that most of the particles flatten out after impinging and show a lamellar structure, while a small fraction of particles is unmelted or just partially melted. The unmelted particles have a distribution in their sizes.

We can see from this section that the surface contains large amounts of oxides with a dual-scale morphology. Oxides have a relatively high surface energy and are usually hydrophilic. On the other hand, the surface roughness may contribute positively to hydrophilicity. Generally, a water droplet on a rough surface is often modeled by Wenzel or Cassie theory (Ref 18). In the Wenzel state the liquid fills the grooves on the rough

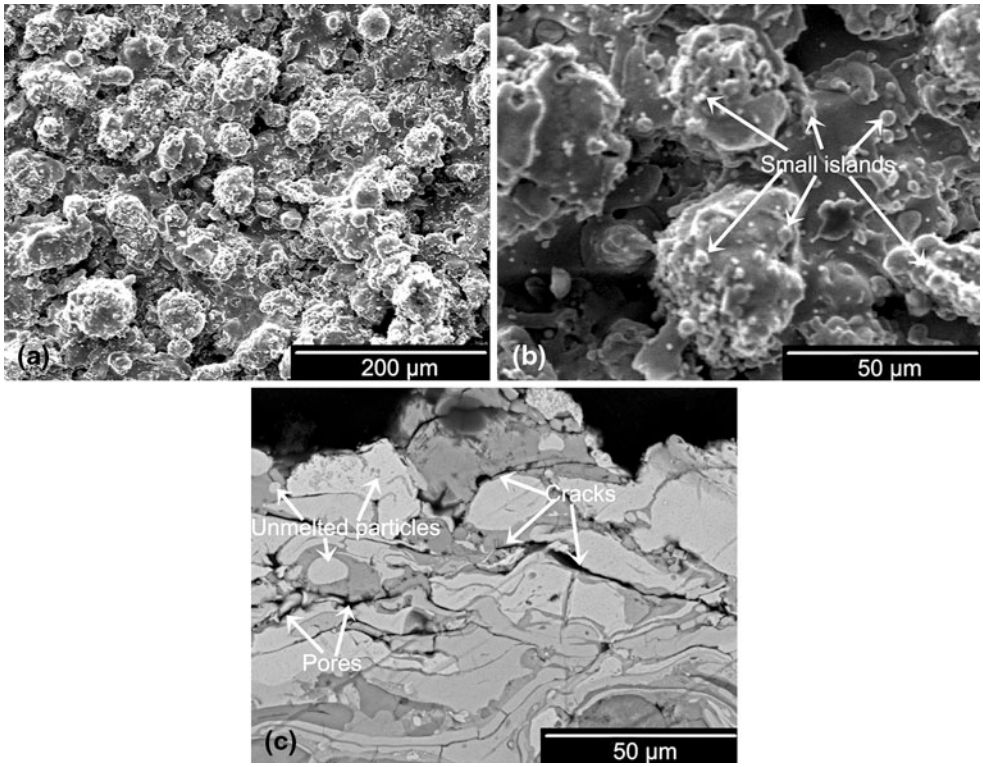

Fig. 4 (a) Morphology of the plasma sprayed mixture coating, (b) a local magnification of (a), and (c) the cross section image (backscattered electron image)

surface. In this case the surface roughness has an amplification effect on hydrophilicity. In Cassie state the liquid does not fill the grooves and thus form a composite surface, and in this case the surface roughness has an amplification effect on hydrophobicity. According to previous study (Ref 19), if the surface energy is high, the wetting state is more in favor of the Wenzel state. Immediately after plasma spraying, the surface is mainly composed of metal oxides with high surface energy. The carbon material adsorbed from air is not enough to cover the entire surface or shield the hydrophilicity of the underlying surface. The intrinsic hydrophilicity of the underlying surface is then amplified by the dual scale roughness, according to the Wenzel theory, which clearly explains the initial superhydrophilicity of the prepared coating.

3.3 Explanation of the Formation of Dual Scale Structure

Although the detailed formation mechanism of the dual scale structure as observed in Fig. 4 is not totally clear at the moment, the particle size distribution of the powders is thought to be an important factor. If the bigger particles in the mixture are not fully melted, then the solidification of such partial-molten particles upon impinging with the substrate will lead to the formation of big islands. On the other hand, the splashing of the fully molten particles upon impinging with the substrate will lead to the formation of smaller islands (Ref 12, 20). Also, some tiny particles in the mixture powders may not be able to penetrate into the flame center (Ref 21, 22) and therefore are not fully melted due to low flame temperature, which would be another reason for the formation of smaller islands.

To verify this hypothesis, the morphology of the coatings prepared by pure metals was investigated, as shown in Fig. 5. From Fig 5(a) and (b), we can see that the surfaces of the sprayed Fe and Cr coatings are relatively smooth, with no big islands. Many small droplets on the surfaces can be ascribed to the splashing of the fully melted particles on the substrates. The lamellar structure of these two coatings, as represented in Fig. 5(c) the structure of Fe, further indicates that these two feedstock powders can be fully melted under the selected conditions. Conversely, we can see from Fig. 5(d) that the surface of the sprayed Ni coating is composed of many bigger round particles. Such morphology indicates that many Ni particles in the feedstock are not fully melted under the selected spraying parameters.

It has been reported (Ref 21, 23–25) that the feedstock particle size has an immense effect on the microstructure of plasma sprayed coatings. Under certain spraying conditions, only the particles within a certain size range can be fully melted and form disc splats. The particles with sizes out of the range cannot be fully melted, which will introduce unmelted particles into the coating (also the islands on the surface). Unmelted particles are serious defects in thermal spray coatings, because they can lead to many other microdefects such as pores and cracks (Ref 6,

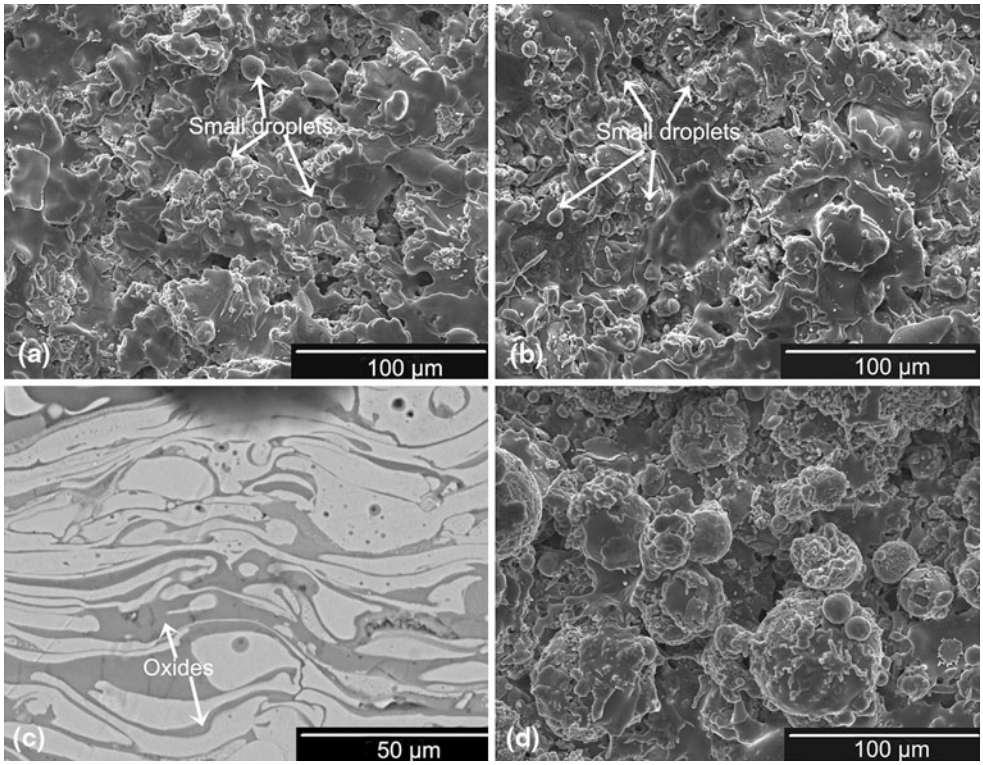

Fig. 5 (a) Morphology of the plasma sprayed Fe coating, (b) morphology of the sprayed Cr coating, (c) a typical cross section image of sprayed Fe coating, and (d) morphology of the sprayed Ni coating

26), as shown in Fig. 4(c). These microdefects are detrimental to mechanical properties of the coatings but beneficial to superhydrophobicity, which will be discussed in detail later.

3.4 Surface Composition Change with Time

As we all know, the wettability of a surface is governed by surface composition and surface morphology (microstructure). Due to the fact that the morphology of the prepared coatings does not change with time, the wettability change can only be ascribed to the surface energy change. There must be some low surface energy materials accumulated on the surface. Based on the XPS results, we found that the only probable low surface energy materials are carbon materials, as shown in Fig. 3 and 6. With the C 1s peak being calibrated using the O 1s peak, the atom fraction of carbon in the mixture coating surface increases from 0.16, several hours after plasma spraying, to 0.55, 60 days after exposure in air. Although the morphology of the coating surface may interfere with the XPS intensity, the macro morphology of the coating is relatively homogenous and the detected area is large enough, plus that several repeated experiments showed the same trend, we think the results shown in Fig. 3 and 6 are relatively credible.

The deconvolution spectrum of the C 1s XPS spectrum (Fig. 7) shows that the C 1s of the specimen includes four absorption peaks, C (284.5 eV), C-H (285.0 eV), C-O (285.6 eV) and C=O (288.2 eV). The existence of C-H,

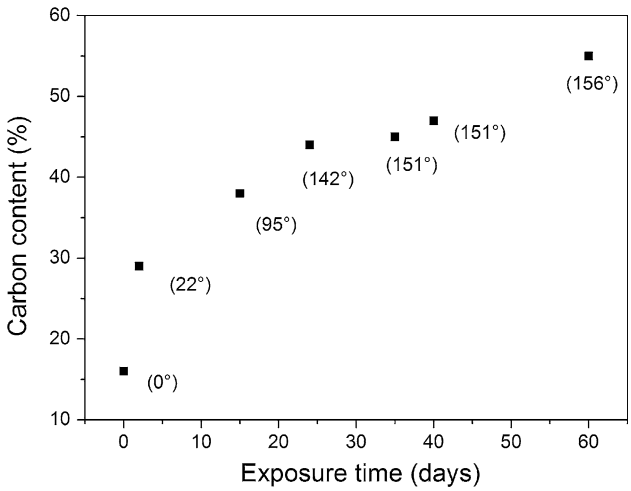

Fig. 6 Carbon content evolution with time. The inset data shows the contact angle corresponding to different exposure time (carbon content)

C-O and C=O peaks indicates the existence of organic pollutants by the adsorption of organic substances from the atmosphere. Previous studies (Ref 16, 17, 27) have confirmed that metal or metal oxide can spontaneously adsorb organic materials from air and lead to the decrease of their surface energy. This adsorption, however, is usually not enough to transform a hydrophilic solid surface to a superhydrophobic one. The C (284.5 eV) peak, we

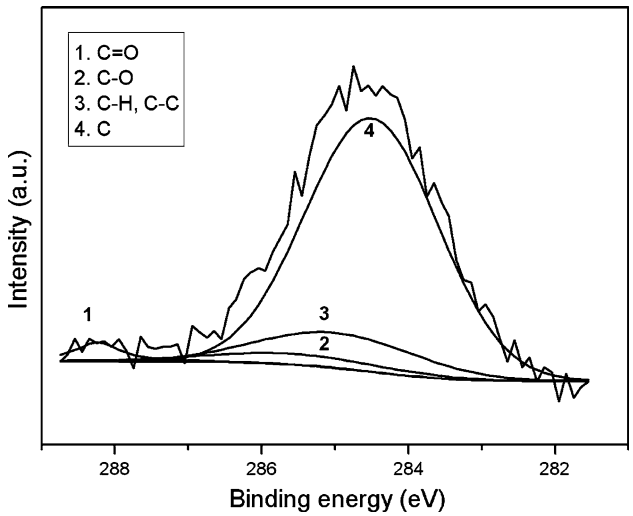

Fig. 7 Peak deconvolution analysis of the XPS for C1s after the spraying process

propose, originates from two reasons: the C-C bond of the organic material, and the decomposition of carbon dioxide by active ferrites.

3.5 Exploration of Carbon Dioxide Decomposition Mechanism

It is already known that active ferrites such as active magnetite $Fe_3O_{4-\delta}$ ($0 < \delta < 1$) and active wustite can catalyze carbon dioxide into zero valence carbon even at room temperature, and change to cation-deficient ferrites because of gradual oxidation (Ref 28–30). Active ferrites are usually prepared by partial reduction of ferrites in hydrogen (Ref 29, 31, 32). Recently it is shown that a laser irradiation can also produce active ferrites (Ref 33). The technique used in this paper, plasma spraying, is similar to laser irradiation in terms of the rapid melting and rapid solidification of metals. It is reasonable to think that during a rapid melting and solidification process, metal will suffer different levels of oxidation, and produce oxygen-deficient oxides due to the difficulty of receiving sufficient oxygen. Do these active ferrites exist in the plasma sprayed surfaces? To explore this, high-resolution XPS of Fe $2p_{3/2}$ and XRD spectrum of the sprayed Fe coating were obtained shortly after spraying, as shown in Fig. 8(a) and 8(b). It can be seen that besides a small fraction of zero valence, the Fe element also stays in different oxidized states, which indicates that the Fe element suffered different levels of oxidation during plasma spraying.

To further support this hypothesis, all the prepared coatings were placed in pure CO_2 and pure Ar atmosphere, respectively, immediately after the plasma spraying. From Table 3, we can see only the sprayed Fe coating and the mixture coating placed in pure CO_2 show a significant change in contact angle. All the other samples have only a slight increase in contact angle. Obviously, heating can speed up the increase of water contact angle on the Fe or mixture coating in pure CO_2. Previous studies (Ref 28–32) have confirmed that carbon dioxide can be

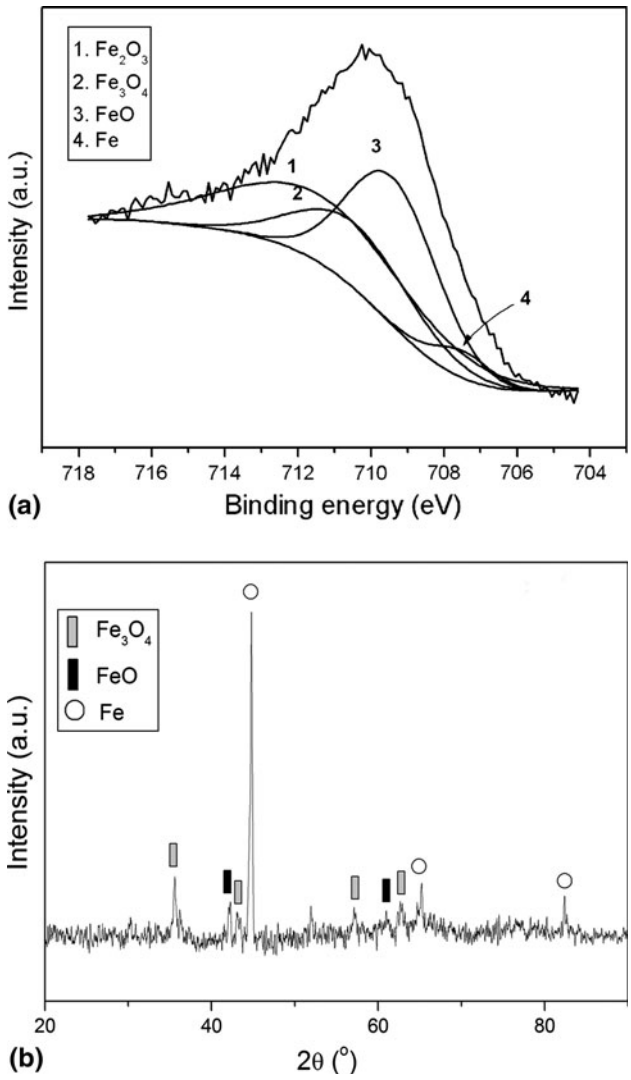

Fig. 8 (a) Peak deconvolution analysis of the XPS for Fe $2p_{3/2}$ and (b) the XRD spectra of the spayed Fe coating shortly after the spraying process

rapidly decomposed into zero valence carbon by active ferrites under a high temperature. The results of our experiment can be reasonably explained by the existence of active ferrites. The existence of zero valence carbon leads to the decrease of surface energy and thus the increase of contact angle.

3.6 The Explanation of the Surface Wettability Change

Immediately after the plasma spraying, the surface of the sprayed metal coatings is mainly composed of metal and metal oxide, both of which have a high surface energy. According to the Wenzel theory, surface roughness can amplify the surface hydrophilicity, so water droplets are found to wet completely all the metallic coatings. As the time elapses, the carbon content in the surface increases (and accordingly the surface energy decreases), which results in the increase of the contact angle as shown in

Table 3 The contact angle of the prepared coatings after treatment in different conditions

Coating	Contact angle			
	No treatment	In Ar, at 583 K, for 7 h	In CO_2, at 583 K, for 7 h	In CO_2, at room temperature, for 10 days
Fe	~0°	<10°	~121°	~73°
Cr	~0°	<15°	<15°	~26°
Ni	~0°	<8°	<8°	~18°
Mixture	~0°	<5°	~105°	~52°

Fig. 6. The deposition of zero valence C as a result of CO_2 decomposition is one important source of carbon accumulation. The superhydrophobicity achieved on the sprayed Fe, Ni and Cr mixture coating is mainly attributed to its double scale roughness (microstructure) and its low surface energy. It has been proven that a dual scale roughness is very crucial for achieving superhydrophobicity (Ref 14, 34, 35). In addition, the cracks and pores are also beneficial to the superhydrophobicity of the mixture coating, owing to the fact that they can store air and increase the air-liquid interface fraction of the composite interface. The increasing of air-liquid interface is preferential to the Cassie state, which makes the water droplet a spherical shape on the surface, and ready to roll off the surface rapidly when slightly tilting the coating.

In Fig.1 we can see that the CA values of the un-polished coatings increase at a relatively slower rate in the initial stage, comparing to those of the polished ones. As explained earlier in this paper, surface roughness can amplify the surface wettability. In the initial stage, the deposition of carbon materials is not enough for achieving hydrophobicity, so the surface roughness may amplify the hydrophilicity and make the CA value on the rough surfaces lower than that on the polished ones. When the deposition of surface carbon materials is high enough for achieving hydrophobicity, the surface roughness may further amplify this hydrophobicity. On the other hand, polishing the surface may also remove most of the surface oxides, and therefore the capture and decomposition of carbon dioxide is also minimized. The lowering of surface energy of the polished surfaces is mainly due to the adsorption of organic materials from the air. This is also an important reason why the CA values on the polished surfaces are all lower than 90°.

4. Conclusion

Wetting behaviors of plasma sprayed Fe, Ni, Cr and their mixture metallic coatings were investigated in this paper. The Fe, Ni and Cr metal powders suffer severe oxidation during plasma spraying. The feedstock particle size distribution has a great influence on the morphology of the coatings. By mixing metal powders with different sizes, plasma spraying can introduce a dual-scale micro/submicro morphology to the surface. The carbon content in the surface is found increasing with time. Besides the already known mechanism of surface adsorption of organic substances, it is found in this paper that the rapid melting and solidification of metals during plasma spraying can produce active ferrites which can capture carbon dioxide from air and decompose it into solid carbon. The accumulated carbon can effectively shield the surface and remarkably increase the contact angle. On the basis of surface dual scale structures, the carbon layer eventually induces superhydrophobicity to the mixture Fe-Ni-Cr coating.

Acknowledgments

This work was supported by the Doctoral Fund of Ministry of Education of China (No. 20110007110009).

References

1. S. Brossard, P.R. Munroe, A.T.T. Tran, and M.M. Hyland, Effects of Substrate Roughness on Splat Formation for Ni-Cr Particles Plasma Sprayed onto Aluminum Substrates, *J. Therm. Spray Technol.*, 2010, **19**(5), p 1131-1141
2. H. Skulev, S. Malinov, W. Sha, and P. Basheer, Microstructural and Mechanical Properties of Nickel-Base Plasma Sprayed Coatings on Steel and Cast Iron Substrates, *Surf. Coat. Technol.*, 2005, **197**(2-3), p 177-184
3. Z. Yin, S. Tao, X. Zhou, and C. Ding, Microstructure and Mechanical Properties of Al_2O_3-Al Composite Coatings Deposited by Plasma Spraying, *Appl. Surf. Sci.*, 2008, **254**(6), p 1636-1643
4. S. Brossard, P.R. Munroe, A.T.T. Tran, and M.M. Hyland, Study of the Splat Microstructure, Splat-Substrate Interface, and the Effects of Substrate Heating on the Splat Formation for Ni-Cr Particles Plasma Sprayed on to Aluminum Substrates, *J. Therm. Spray Technol.*, 2010, **19**(5), p 1115-1130
5. X.C. Zhang, B.S. Xu, F.Z. Xuan, H.D. Wang, and Y.X. Wu, Microstructural and Porosity Variations in the Plasma-Sprayed Ni-Alloy Coatings Prepared at Different Spraying Powers, *J. Alloys Compd.*, 2009, **473**(1-2), p 145-151
6. Z. Zhou, L. Wang, D.Y. He, F.C. Wang, and Y.B. Liu, Microstructure and Electrochemical Behavior of Fe-Based Amorphous Metallic Coatings Fabricated by Atmospheric Plasma Spraying, *J. Therm. Spray Technol.*, 2010, **20**(1-2), p 344-350
7. X.C. Zhang, B.S. Xu, F.Z. Xuan, S.T. Tu, H.D. Wang, and Y.X. Wu, Porosity and Effective Mechanical Properties of Plasma-Sprayed Ni-Based Alloy Coatings, *Appl. Surf. Sci.*, 2009, **255**(8), p 4362-4371
8. S. Brossard, P.R. Munroe, A.T. Tran, and M.M. Hyland, Study of the Splat Microstructure and the Effects of Substrate Heating on the Splat Formation for Ni-Cr Particles Plasma Sprayed onto Stainless Steel Substrates, *J. Therm. Spray Technol.*, 2010, **19**(5), p 1100-1114
9. P. Ctibor, K. Neufuss, and P. Chraska, Microstructure and Abrasion Resistance of Plasma Sprayed Titania Coatings, *J. Therm. Spray Technol.*, 2006, **15**(4), p 689-694

10. H. Du, J.H. Shin, and S.W. Lee, Study on Porosity of Plasma-Sprayed Coatings by Digital Image Analysis Method, *J. Therm. Spray Technol.*, 2005, **14**(4), p 453-461
11. L.D. Zhao and E. Lugscheider, Influence of the Spraying Processes on the Properties of 316L Stainless Steel Coatings, *Surf. Coat. Tech.*, 2003, **162**(1), p 6-10
12. Z. Zeng, S. Kuroda, and H. Era, Comparison of Oxidation Behavior of Ni-20Cr Alloy and Ni-Base Self-Fluxing Alloy During Air Plasma Spraying, *Surf. Coat. Technol.*, 2009, **204**(1-2), p 69-77
13. Z. Guo, W. Liu, and B.-L. Su, Superhydrophobic Surfaces: From Natural to Biomimetic to Functional, *J. Colloid Interface Sci.*, 2011, **353**(2), p 335-355
14. B. Bhushan and Y.C. Jung, Natural and Biomimetic Artificial Surfaces for Superhydrophobicity, Self-Cleaning, Low Adhesion, and Drag Reduction, *Prog. Mater Sci.*, 2011, **56**(1), p 1-108
15. Y.G. Guo, Q.H. Wang, and T.M. Wang, Facile Fabrication of Superhydrophobic Surface with Micro/Nanoscale Binary Structures on Aluminum Substrate, *Appl. Surf. Sci.*, 2011, **257**(13), p 5831-5836
16. M. Harju, E. Levanen, and T. Mantyla, Wetting Behaviour of Plasma Sprayed Oxide Coatings, *Appl. Surf. Sci.*, 2006, **252**(24), p 8514-8520
17. S. Takeda, M. Fukawa, Y. Hayashi, and K. Matsumoto, Surface OH Group Governing adsorption Properties of Metal Oxide Films, *Thin Solid Films*, 1999, **339**, p 220-224
18. C. Dorrer and J. Ruhe, Some Thoughts on Superhydrophobic Wetting, *Soft Matter*, 2009, **5**(1), p 51-61
19. N.A. Patankar, On the Modeling of Hydrophobic Contact Angles on Rough Surfaces, *Langmuir*, 2003, **19**(4), p 1249-1253
20. A.T.T. Tran, M.M. Hyland, T. Qiu, B. Withy, and B.J. James, Effects of Surface Chemistry on Splat Formation During Plasma Spraying, *J. Therm. Spray Technol.*, 2008, **17**(5-6), p 637-645
21. H. Xiong, L. Zheng, L. Li, and A. Vaidya, Melting and Oxidation Behavior of In-Flight Particles in Plasma Spray Process, *Int. J. Heat Mass Transf.*, 2005, **48**(25-26), p 5121-5133
22. P. Fauchais, Understanding Plasma Spraying, *J. Phys. D*, 2004, **37**(9), p R86-R108
23. H. Xiong, L. Zheng, S. Sampath, R. Williamson, and J. Fincke, Three-Dimensional Simulation of Plasma Spray: Effects of Carrier Gas Flow and Particle Injection on Plasma Jet and Entrained Particle Behavior, *Int. J. Heat Mass Transf.*, 2004, **47**(24), p 5189-5200
24. P. Fauchais, G. Montavon, and G. Bertrand, From Powders to Thermally Sprayed Coatings, *J. Therm. Spray Technol.*, 2010, **19**(1-2), p 56-80
25. G. Mauer, R. Vassen, D. Stover, S. Kirner, J.L. Marques, S. Zimmermann, G. Forster, and J. Schein, Improving Powder Injection in Plasma Spraying by Optical Diagnostics of the Plasma and Particle Characterization, *J. Therm. Spray Technol.*, 2011, **20**(1-2), p 3-11
26. X.Q. Liu, Y.G. Zheng, X.C. Chang, W.L. Hou, J.Q. Wang, Z. Tang, and A. Burgess, Microstructure and Properties of Fe-Based Amorphous Metallic Coating Produced by High Velocity Axial Plasma Spraying, *J. Alloys Compd.*, 2009, **484**(1-2), p 300-307
27. B. Yan, J. Tao, C. Pang, Z. Zheng, Z. Shen, C.H.A. Huan, and T. Yu, Reversible UV-Light-Induced Ultrahydrophobic-to-Ultrahydrophilic Transition in an α-Fe_2O_3 Nanoflakes Film, *Langmuir*, 2008, **24**(19), p 10569-10571
28. Y. Tamaura and M. Tabata, Complete Reduction of Carbon Dioxide to Carbon Using Cation-Excess Magnetite, *Nature*, 1990, **36**, p 255
29. C.-l. Zhang, S. Li, L.-j. Wang, T.-h. Wu, and S.-y. Peng, Studies on the Decomposition of Carbon Dioxide into Carbon with Oxygen-Deficient Magnetite: I. Preparation, Characterization of Magnetite, and Its Activity of Decomposing Carbon Dioxide, *Mater. Chem. Phys.*, 2000, **62**(1), p 44-51
30. C.-L. Zhang, S. Li, T.-H. Wu, and S.-Y. Peng, Reduction of Carbon Dioxide into Carbon by the Active Wustite and the Mechanism of the Reaction, *Mater. Chem. Phys.*, 1999, **58**(2), p 139-145
31. M.H. Khedr, M. Bahgat, M.I. Nasr, and E.K. Sedeek, CO_2 Decomposition over Freshly Reduced Nanocrystalline Fe_2O_3, *Colloids Surf. A*, 2007, **302**(1-3), p 517-524
32. M.H. Khedr, A.A. Omar, and S.A. Abdel-Moaty, Reduction of Carbon Dioxide into Carbon by Freshly Reduced $CoFe_2O_4$ Nanoparticles, *Mater. Sci. Eng, A*, 2006, **432**(1-2), p 26-33
33. A.M. Kietzig, S.G. Hatzikiriakos, and P. Englezos, Patterned Superhydrophobic Metallic Surfaces, *Langmuir*, 2009, **25**(8), p 4821-4827
34. L.C. Gao and T.J. McCarthy, The "Lotus Effect" Explained: Two Reasons Why Two Length Scales of Topography are Important, *Langmuir*, 2006, **22**(7), p 2966-2967
35. M. Nosonovsky, Multiscale Roughness and Stability of Superhydrophobic Biomimetic Interfaces, *Langmuir*, 2007, **23**(6), p 3157-3161